A ROBUST BAYESIAN MULTISENSOR FUSION ALGORITHM FOR JOINT LANE AND PAVEMENT BOUNDARY DETECTION

Bing Ma

Department of EECS
University of Michigan
Ann Arbor, MI 48109, USA

Sridhar Lakshmanan

Department of ECE
University of Michigan – Dearborn
Dearborn, MI 48128, USA

Alfred Hero

Department of EECS
University of Michigan
Ann Arbor, MI 48109, USA

ABSTRACT

In this paper we propose to simultaneously detect lane and pavement boundaries by fusing information from both optical and radar images. The boundaries are described with concentric circular models. The optical and radar imaging processes are represented with Gaussian and log-normal probability densities. The multisensor fusion boundary detection problem is posed in a Bayesian framework and a joint maximum *a posteriori* (MAP) estimate is employed to locate the road and lane boundaries. Since the circular model parameters are expressed in compatible units, the estimation problem is much better conditioned than using the previous parabolic models. Experimental results are shown to demonstrate that the fusion algorithm outperforms single sensor based boundary detection algorithms in a variety of road scenarios.

1. INTRODUCTION

Automated detection of lane and pavement boundaries is an enabling or enhancing technology in developing the next generation of automotive systems. It will provide necessary information for road departure or lane excursion warning, intelligent cruise control, and ultimately, autonomous driving.

In recently years, boundary detection has been broadly studied and many state-of-the-art systems for detecting and tracking lane/pavement boundaries use *a priori* deformable templates (shape models) to mathematically describe the appearance of these boundaries [1, 2, 3, 4]. The boundary detection approaches via deformable templates outperform the conventional edge based techniques due to their robustness to noise and their capability of rejecting false boundaries (such as entry/exit ramps).

Kluge and Lakshmanan presented a deformable template algorithm to detect lane boundaries in optical images [2]. Ma, Lakshmanan, and Hero proposed an algorithm to detect pavement boundaries in radar images [3]. In both applications, the lane and pavement boundaries were described with parabolic shape models and the optical and radar imaging processes were represented by empirical non-normalized matching functions and log-normal densities. The boundary detection problems were solved by estimating the shape parameters with maximum *a posteriori* method.

In an extensive boundary detection experiment carried on a large number of optical and radar images, it has been observed that in some cases, single sensor based boundary detection algorithms fail to correctly locate the lane or pavement boundaries due to poor quality of the optical or radar images. The reason behind this failure is that a single sensor, either optical or radar sensor, limits itself in the ability to sense and identify the relevant features in varying environments. For example, the optical sensor is not able to operate effectively in a poorly illuminated environment, while the radar sensor can not distinguish the lane markers on the road. To take advantage of the strengths (and overcome the weaknesses) of both the optical and radar sensors, we propose to combine the two different types of sensory data together since multiple sensors will provide more information and hence a better and more precise interpretation of the sensed environment.

In [4] we investigated a multisensor fusion technique to simultaneously detect lane and pavement boundaries in optical and radar images. This fusion technique made use of existing prior and likelihood models presented in [2, 3]. Since this fusion technique integrates information from both optical and radar images, the boundary detection results were shown to be more accurate and more reliable than single sensor based detection algorithms, especially in an adverse environment.

Although the detection results of [4] remain promising, there are some drawbacks that prevent us from getting the most out of the fusion algorithm. First, since the parameters in the parabolic shape model have different units and are of different orders of magnitude, the MAP estimation problem is an inherent ill conditioned problem[5]. To eliminate this inherent pitfall of the parabolic model, in this paper we propose to use concentric circular shape models to describe the lane and pavement boundaries. Circular shape models lead to a better conditioned estimation problem due to the compatibility of their parameters, namely, parameters share the same units and are of the same orders of magnitude over ranges of interest.

Second, the existing optical likelihood function results in complications in the joint estimation problem. The empirical matching function used in the single optical sensor lane detection algorithm [2] is not a valid likelihood function since it is not normalized to a probability density function (pdf). In the radar and optical fusion algorithm, the empirical function has to be carefully weighted so that each sensor makes a balanced contribution to the joint likelihood. In [4] we experimentally selected the weights which yield reasonably good results, but this empirical matching function make systematic and theoretically sound weight picking a difficult task. Inspired by the log-normal radar imaging likelihood function, we propose to model the optical imaging process as a Gaussian process which leads to a well defined likelihood function that can be easily manipulated with the likelihood from the radar sensor.

In the improved fusion algorithm proposed in this paper, we employ concentric circular shape models to represent the lane and pavement boundaries, and utilize the Gaussian and log-normal pdf's to describe the radar and optical imaging processes. This new fusion algorithm is expected to yield a well conditioned estimation problem and combines the optical and radar modalities both effectively and efficiently.

2. CONCENTRIC CIRCULAR MODELS

In [5] we proposed using concentric circular shape models to describe the pavement boundaries in radar images, which resulted in a better conditioned estimation problem than previous parabolic shape models. In this paper, we shall use circular shape models to describe both pavement and lane boundaries on the ground plane. A typical road scenario can be modeled by an intersection of a cone with two concentric circles (Fig. 1). The cone represents the field-of-view of the sensor, and the two circles represent the left and right pavement/lane boundaries.

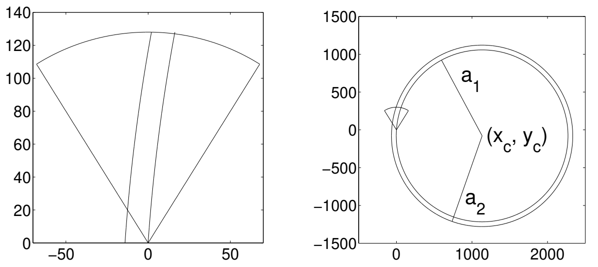

(a) Field-of-view of the sensor (b) Complete circular shape model

Fig. 1. A typical road scenario in a radar image

Assuming that the apex of the cone is at the origin $(0, 0)$, we represent the coordinates (x, y) of the pavement(lane) boundaries by arcs of circles centered at (x_c, y_c) with radii a_1 and a_2 (a_3 and a_4), respectively

$$(x - x_c)^2 + (y - y_c)^2 = (a_{1,2})^2 . \qquad (1)$$

Denote by $\underline{\theta}_c^r = \{x_c, y_c, a_1, a_2\}$ the shape parameters for the pavement boundaries, and by $\underline{\theta}_c^o = \{x_c, y_c, a_3, a_4\}$ the shape parameters for the lane boundaries. Note that the lane and pavement boundaries share the same parameters x_c and y_c and the only parameter that distinguishes the boundaries is the radius $a_i, i = 1, 2, 3, 4$.

The domain of the optical image is a perspective projection of the road scenario on the ground plane. To make the optical observation data accordant with the boundary shape models, we project the optical image data onto the ground plane with the inverse perspective projection [6].

There are some prior constraints on the lane and pavement boundary parameters: (1) the circles must intersect the cone; (2) the host vehicle (the apex of the cone) is within the road; (3) the lane is positioned inside the road region; and (4) the lane/pavement width has to be within minimum and maximum limits. These constraints can be expressed by introducing the prior density on the boundary parameters $\underline{\theta}_c = \{\underline{\theta}_c^r, \underline{\theta}_c^o\}$:

$$\begin{aligned} P(\underline{\theta}_c) &= \frac{1}{\gamma_c} \cdot I_{[a_1-p_1, a_2+p_2]}(x_c^2 + y_c^2) \\ &\cdot I_{[\alpha_{min}, \alpha_{max}]}\left(\text{atan}\left(\frac{y_c}{x_c}\right)\right) \cdot I_{[a_1, a_2']}(a_1') \cdot I_{[a_1', a_2]}(a_2') \\ &\cdot I_{[W_{min}, W_{max}]}(a_2 - a_1) \cdot I_{[W'_{min}, W'_{max}]}(a_2' - a_1') \qquad (2) \end{aligned}$$

where γ_c is a normalizing constant and $I_A(x)$ is an indicator function of set A,

$$I_A(x) = \begin{cases} 1, & \text{if } x \in A \\ 0, & \text{otherwise} \end{cases}$$

This prior pdf is simply a uniform distribution over the space of feasible model parameters.

3. IMAGING LIKELIHOODS

3.1. Radar Imaging Likelihood

We model the radar imaging process by the log-normal pdf presented in [3]. For the radar image Z^r, the radar imaging likelihood is described using the conditional probability that the random field Z^r takes on a realization z^r (corresponding to the radar observation), given that the pavement boundary information $\underline{\theta}_c^r$ is known,

$$\begin{aligned} p(z^r \mid \underline{\theta}_c^r) &= \prod_{(x,y)\in\mathcal{L}} \frac{1}{z_{xy}^r \sqrt{2\pi\sigma_{xy}^2(\underline{\theta}_c^r)}} \\ &\exp\left\{-\frac{1}{2\sigma_{xy}^2(\underline{\theta}_c^r)}\left[\log z_{xy}^r - \mu_{xy}(\underline{\theta}_c^r)\right]^2\right\} \qquad (3) \end{aligned}$$

3.2. Optical Imaging Likelihood

For a noiseless optical image containing ideal lane boundaries, the gradient magnitudes at the pixels which lie on the boundaries have the maximum value, and the gradient magnitudes taper to zero as the pixels get further away from the boundaries. So the ideal gradient magnitudes constitute a tapered image $S(\underline{\theta}_c^o)$. Define the taper function

$$f(\alpha, d) \triangleq \frac{1}{1+\alpha d^2}, \tag{4}$$

where α is a constant which controls the effective width of the taper function. Then the intensity value of the tapered image at the pixel (x, y), $S(\underline{\theta}_c^o, x, y)$, can be written as

$$(\underline{\theta}_c^o, x, y) = A\ f(\alpha, d_1(x, y)) + A\ f(\alpha, d_2(x, y)) \tag{5}$$

where A is the maximum gradient magnitude and d_1 and d_2 are the distances from the pixel (x, y) to the left and right lane boundaries, respectively.

Given lane boundary shape parameters $\underline{\theta}_c^o$, we assume that the optical image gradient magnitude G_m is the ideal gradient magnitude $S(\underline{\theta}_c^o)$ contaminated with additive white Gaussian noise W^o,

$$G_m = S(\underline{\theta}_c^o) + W^o, \tag{6}$$

where W^o are i.i.d. Gaussian random variables with mean 0 and unknown variance σ^2. Thus the optical imaging process is a realization of the conditional density of the optical random field Z^o taking a realization z^o given the lane boundary information $\underline{\theta}_c^o$. This can be modeled as a Gaussian pdf,

$$p(z^o|\underline{\theta}_c^o) = \prod_{(x,y)} \frac{1}{\sqrt{2\pi\sigma^2}} \exp\left\{ -\frac{[g_m(x,y) - S(\underline{\theta}_c^o, x, y)]^2}{2\sigma^2} \right\} \tag{7}$$

4. MULTISENSOR FUSION METHOD — JOINT MAP ESTIMATE

Since the prior distributions of the deformation parameters and the imaging likelihood functions are available, we shall pose the lane and pavement boundary detection problem in a Bayesian framework. The optical and radar fusion detection problem can be solved by estimating the deformation parameters $\underline{\theta}_c$ with the joint maximum *a posteriori* estimate

$$\hat{\underline{\theta}}_c = \arg\max_{\underline{\theta}_c} P(\underline{\theta}_c | z^r, z^o)$$

Utilizing the Bayes' rule and the fact that $P(z^r, z^o)$ is fixed by the observation, we have

$$\hat{\underline{\theta}}_c \quad = \quad \arg\max_{\underline{\theta}_c} P(z^r, z^o, \underline{\theta}_c) \tag{8}$$

By the chain rule of conditional probability,

$$P(z^r, z^o, \underline{\theta}_c) = P(\underline{\theta}_c^r) P(z^r|\underline{\theta}_c^r) P(\underline{\theta}_c^o|\underline{\theta}_c^r, z^r) P(z^o|\underline{\theta}_c^o, z^r, \underline{\theta}_c^r) \tag{9}$$

Since the radar and optical imaging processes are independent, the optical parameters $\underline{\theta}_c^o$ are conditionally independent of the radar observation z^r given the radar parameters $\underline{\theta}_c^r$, and the optical observation z^o is conditionally independent of the radar observation z^r and radar parameters $\underline{\theta}_c^r$ given the optical parameters $\underline{\theta}_c^o$, that is,

$$\begin{aligned} P(\underline{\theta}_c^o | \underline{\theta}_c^r, z^r) &= P(\underline{\theta}_c^o | \underline{\theta}_c^r) \\ P(z^o | \underline{\theta}_c^o, z^r, \underline{\theta}_c^r) &= P(z^o | \underline{\theta}_c^o) \end{aligned} \tag{10}$$

Combining Eqns. (8), (9) and (10) yields

$$\hat{\underline{\theta}}_c = \arg\max_{\underline{\theta}_c} P(\underline{\theta}_c)\ P(z^r|\underline{\theta}_c^r)\ P(z^o|\underline{\theta}_c^o) \tag{11}$$

5. EXPERIMENTAL RESULTS

We have implemented the proposed joint boundary detection algorithm (11) to locate lane and pavement boundaries in registered optical and radar images. We have also implemented the single sensor based lane/pavement boundary detection algorithms for comparison. In the single sensor based algorithms, we also represent the boundaries with circular shape models and describe the optical and radar imaging processes with Gaussian and log-normal densities.

In Fig. 2 we show detection results for a pair of optical and radar images of different qualities. The optical image is degraded by the presence of snow. Wrong lane boundary detection result is obtained when only the optical image is used (Fig. 2(a)). However, the radar image still offers sufficient information to correctly detect the pavement boundaries (Fig. 2(b)). In the fusion approach, since we make use of information from both optical and radar sensors to jointly detect the lane and pavement boundaries, the radar image helps refine and improve the lane detection in the optical images (Figs. 2(c) and (d)).

In Fig. 3 we show detection results for a pair of fair-quality optical and bad-quality radar images. The single sensor based algorithms do not operate well in either lane or pavement boundary detection. Fig. 3(a) gives the lane detection result in the optical image. The traffic sign to the right of the road misleads the algorithm to produce boundaries curving to the left. In Fig. 3(b), a homogeneous region to the left of the road results in wrong pavement boundaries. Information from both optical and radar images is explored in the fusion approach and the redundancy and complementarity between the optical and radar sensors significantly improve the boundary detection performance. In Figs. 3(c) and (d), we show that satisfactory results have been achieved with the joint boundary detection algorithm.

Since the parameters of circular shape models have the same units and are of the same orders of magnitude, the estimation problems are much better conditioned than parabolic models. Take the estimation problem in Fig. 3 as an example, the condition number is 13.24 for the circular shape model and is 8.68×10^6 for the parabolic shape model.

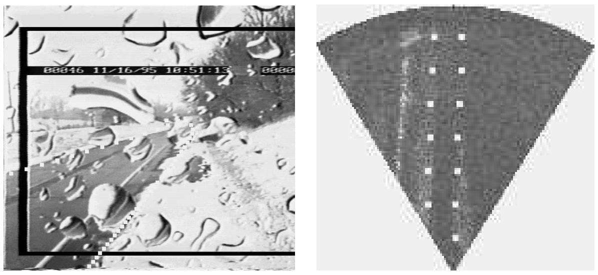

(a) Single sensor based detection (b) Single sensor based detection

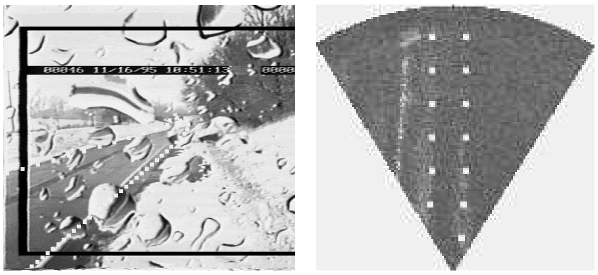

(c) Detection with fusion method (d) Detection with fusion method

Fig. 2. Performance comparison of the fusion and single sensor based methods

In this fusion algorithm, the background noise levels are assumed unknown in both radar and optical imaging likelihoods and hence the MAP estimates of the shape parameters are log quadratic in the observations for both modalities. Unlike in [4], the background noise level is assumed unknown in the radar imaging likelihood and known in the optical imaging likelihood and hence the MAP estimates of the shape parameters are log quadratic in the radar observations but linear in the optical observations. Since the optical and radar imaging likelihoods proposed in this paper are compatible, no ad hoc weighting scheme is necessary as in [4]. We applied both fusion algorithms proposed in this paper and in [4] to a database of 25 optical and radar image pairs obtained in various illuminating environments. The average detection error standard deviations are plotted in Fig. 4. Both Figs. 4(a) and (b) demonstrate that the new fusion algorithm outperforms the previous fusion algorithm in detecting the lane and pavement boundaries.

The experiments have demonstrated that circular shape models and the newly formulated radar and optical likelihoods are indeed successful in detecting lane and pavement boundaries.

6. REFERENCES

[1] *Proc. IEEE Intelligent Vehicles Symposium*, 1998.

[2] K. C. Kluge and S. Lakshmanan, "A deformable-template approach to lane detection," in *Proc. IEEE Intell. Vehic. Symp.*, Sept. 1995.

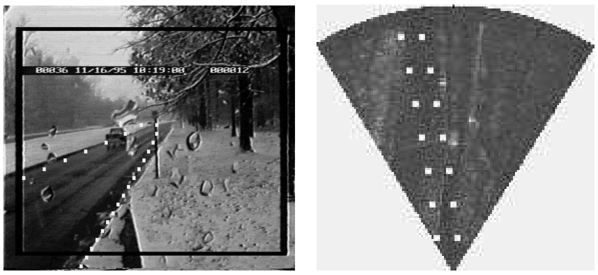

(a) Single sensor based detection (b) Single sensor based detection

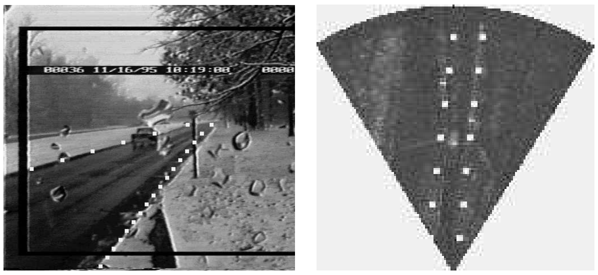

(c) Detection with fusion method (d) Detection with fusion method

Fig. 3. Performance comparison of the fusion and single sensor based methods

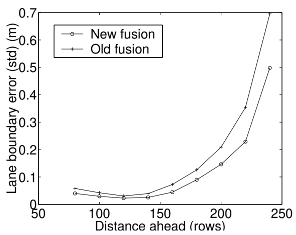

(a) Errors for lane boundary detection

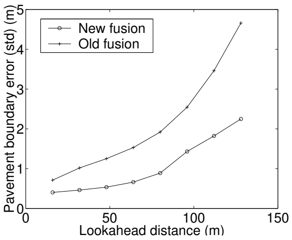

(b) Errors for pavement boundary detection

Fig. 4. Performance comparison of fusion algorithms

[3] B. Ma, S. Lakshmanan, and A. Hero, "Detection of curved road edges in radar images via deformable templates," in *Proc. IEEE. Intl. Conf. Image Proc.*, 1997.

[4] B. Ma, S. Lakshmanan, and A. Hero, "Simultaneous detection of lane and pavement boundaries using model-based multisensor fusion," *IEEE Trans. Intelligent Transportation Systems*, vol. 1, no. 3, pp. 135–147, Sept. 2000.

[5] B. Ma, S. Lakshmanan, and A. Hero, "Pavement boundary detection via circular shape models," in *Proc. IEEE Intell. Vehic. Symp.*, Dearborn, MI, Oct 2000.

[6] K. Kluge, "Extracting road curvature and orientation from image edge points without perceptual grouping into features," in *Proc. IEEE Intell. Vehic. Symp.*, Paris, Fr., 1994, pp. 109–114.